

pubs.acs.org/acscatalysis Research Article

# Synergistic Excited State Photocatalysis: Divergent Energy Transfer vs Lewis Acid Mediated Phototransformations

Jayachandran Parthiban, Dipti Garg, Sapna Ahuja, Steffen Jockusch, Angel Ugrinov, and Jayaraman Sivaguru\*



Cite This: ACS Catal. 2024, 14, 8794-8802



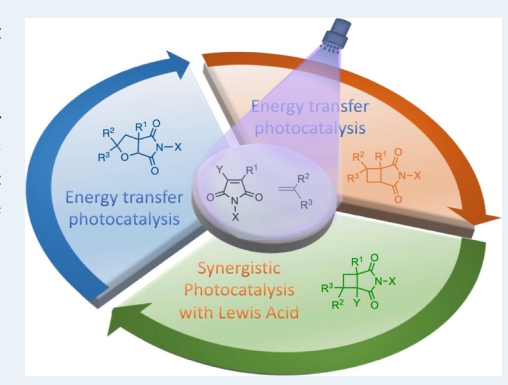
**ACCESS** I

III Metrics & More

Article Recommendations

s Supporting Information

ABSTRACT: Energy transfer vs Lewis acid photocatalysis dependent product selectivity is reported for the photochemical reaction of maleimides with alkenes. The photoproduct selectivity depends on the mode of photocatalysis that was deciphered using photochemical and photophysical studies. Under energy transfer conditions, hydroxy maleimides undergo a [3+2]-photocycloaddition, while in the presence of Lewis acids [2+2]-photocycloaddition was observed. Synergistic interactions between the Lewis acid, triplet sensitizer, and the substrate dictate both the outcome and efficiency of [2+2]-photocycloaddition.



KEYWORDS: synergistic photocatalysis, Lewis acid, chemoselectivity, regioselectivity, photocycloaddition reaction

ynergistic interactions between substrates and catalysts are hallmarks of enzymatic biocatalysis that often features unparalleled rate acceleration in addition to providing access to unique molecular architectures. <sup>1,2</sup> Translating such phenomena to chemical processes is challenging due to the difficulty in altering the reaction trajectories to dictate product outcome with high efficiency.<sup>3</sup> This problem is even more pronounced for excited state transformations where reaction pathways often involve short-lived transient(s) and/or intermediate(s). In spite of this challenge, altering photochemical pathways offer a unique opportunity to modulate excited state reactivities with control over product chemo-, regio-, and stereoselectivities.<sup>4,5</sup> This requires manipulation of excited state dynamics to channel photoreactivity toward a specified reaction trajectory. 6-9 Recent developments in photocatalytic approaches have centered around the development of visible light mediated reactions. 10-15 The prospect of affecting excited state transformation with visible light is both challenging and stimulating due to the energetics and the multiplicity of reactive intermediate(s) involved in the reaction, when compared to ground state thermal/photoredox transformations. Accessing excited states of organic molecules often requires direct excitation in the UVA region that places limitations on the manipulation of their photochemistry.<sup>8,9</sup>

The seminal work of Lewis and co-workers in the early 1980s showed that complexation of reactive substrates with Lewis acids led to a bathochromic shift in absorption profiles of reactive substrates, indicating the lowering of the excited state energies. <sup>16,17</sup> In recent years, <sup>18,19</sup> this has been exploited

by the groups of Bach, <sup>20,21</sup> Yoon, <sup>22–24</sup> and others <sup>25–29</sup> to promote photochemical transformations with high stereoselectivity. One of the salient features in the reported systems is that the same photoproduct is observed both in the presence and in the absence of Lewis acids. <sup>16–29</sup> We were interested in utilizing the Lewis acid complexation to alter the outcome of the reaction by changing the product being formed in the photochemical transformations as we envisioned altering the type of intermediates participating in the reaction pathways. <sup>30</sup> In this report, we disclose our findings with maleimides <sup>31–34</sup> in which the observed photoproduct is dictated by the mode of photocatalysis, viz., energy transfer or Lewis acid photocatalysis (Figure 1).

We began our investigation by evaluating the photoreaction of maleimides 1 with various alkenes 2 (Scheme 1). Direct irradiation ( $\sim 350 \pm 30$  nm) of maleimide 1a with alkene 2a did not lead to any noticeable conversion with complete recovery of the reactants. Photoirradiation at  $\sim 420 \pm 30$  nm (16 h irradiation) of maleimide 1a with alkene 2a with thioxanthone (TX) as a photosensitizer led to an efficient reaction leading to photoproduct 3a in 66% isolated yield

Received: February 24, 2024 Revised: May 10, 2024 Accepted: May 13, 2024



# Synergistic Photocatalysis

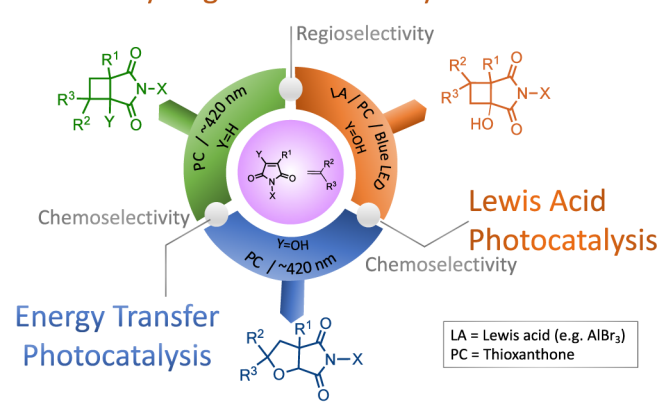


Figure 1. Controlling excited state reactivity via energy transfer vs Lewis acid mediated phototransformations.

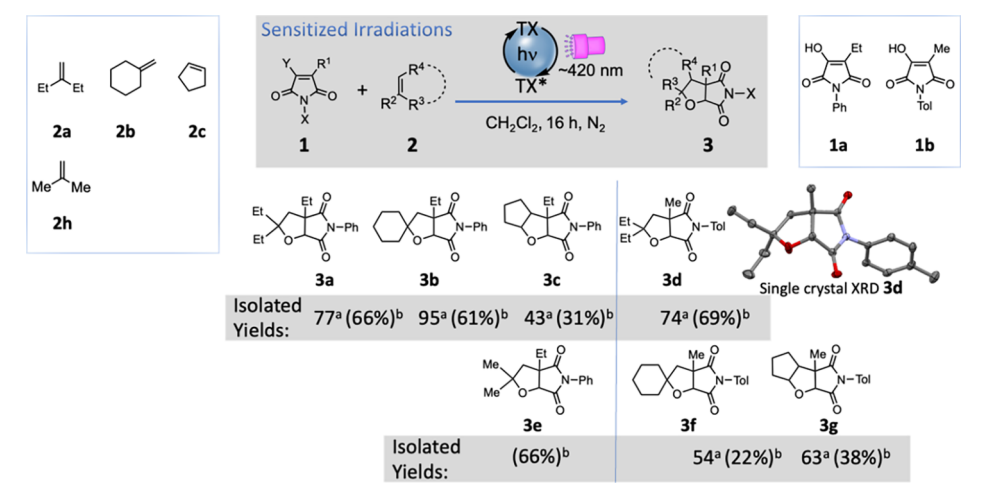
(Scheme 1). The photoproduct was characterized by NMR spectroscopy and HRMS.<sup>35</sup>

The generality of the reaction using thioxanthone sensitizer was established by changing both the maleimide and the alkene.<sup>35</sup> Thioxanthone-sensitized photoreaction of 1a with alkenes 2b and 2c led to the corresponding photoproducts 3b and 3c with yields (by <sup>1</sup>H NMR spectroscopy) of 95% and 43%, respectively. The compounds were isolated in 61% yield (for 3b) and 31% yield (for 3c). Varying the maleimide from 1a to 1b also led to similar reactivity. Thioxanthone-sensitized photoreaction of 1b with alkenes 2a, 2b, and 2c led to the corresponding photoproducts 3d, 3e, 3f, and 3g in yields varying from 74% to 54% (by <sup>1</sup>H NMR spectroscopy; isolated yields varied from 69% to 22%). We were also successful in unambiguously establishing the structure of the photoproduct 3d by single-crystal XRD.<sup>35</sup> In addition, a large-scale photocatalytic reaction under energy transfer sensitization led to efficient [3+2]-photocycloaddition of maleimide 1a (0.5 g scale) and alkene 2a, leading to photoproduct 3a in 57% isolated yield (0.39 g of 3a), showcasing the synthetic utility of the transformations. Due to the structural feature of maleimide 1, we proceeded to investigate the effect of Lewis acids in promoting the phototransformation (Scheme 2). To our

surprise, blue LED irradiation ( $\sim$ 455 ± 20 nm) of 1a and 2a with 50 mol % of AlCl<sub>3</sub> for 24 h led to the formation of photoproduct 4a in 46% isolated yield (Scheme 2, top). The photoproduct was characterized by NMR spectroscopy and HRMS.<sup>35</sup> The structure was unequivocally established by single-crystal XRD (Scheme 2).35 It is critical to note that the chemoselectivity in the photochemical transformations was observed under two different conditions employed, i.e., a [3+2]-type photochemical reaction<sup>36-39</sup> leading to photoproduct 3 under energy transfer conditions and [2+2]photocycloaddition leading to photoproduct 4 under Lewis acid mediated conditions (compare Schemes 1 and 2). To gauge the influence of triplet sensitizers under Lewis acid conditions, we also evaluated the photoreactivity of 1a and 2a in the presence of AlCl<sub>3</sub> and TX. Blue LED irradiation of 1a and 2a with 50 mol % of AlCl<sub>3</sub> and 10 mol % of TX for 5 h led to the formation of photoproduct 4a in 74% isolated yield (Scheme 2, botom). It is critical to note the synergistic effect of both the Lewis acid and the photosensitizer in promoting the transformation and impacting its efficiency and conversions. As shown in Scheme 2, blue LED irradiation in the presence of both the Lewis acid and thioxanthone sensitizer resulted in 74% isolated yield of photoproduct 4a in just 5 h, while 24 h blue LED irradiation was required when Lewis acid alone was employed to promote the reaction, leading to 46% isolated yield. These observations (Schemes 1 and 2) necessitated an in-depth investigation into the role of Lewis acid and the sensitizer in controlling chemoselectivity and promoting the photochemical transformation.

We started our evaluation of the synergistic effect of Lewis acid and the triplet sensitizer on the phototransformation involving 1a and 2a under our standard conditions, viz., 50 mol % Lewis acid and 10 mol % of the thioxanthone sensitizer under blue LED irradiation for 5 h in dichloromethane at room temperature. Changing the Lewis acid from  $AlCl_3$  to  $AlBr_3$  resulted in a minor change in the isolated yield of the photoproduct 4a (from 74% for  $AlCl_3$  to 66% for  $AlBr_3$ ; compare  $Table\ 1$ , entries 1 and 2). Changing the Lewis acid to  $BF_3 \cdot Et_2O$  resulted in 9% isolated yield of the photoproduct 4a ( $Table\ 1$ , entry 3). Due to the significant drop in the isolated yield of the photoproduct 4a upon changing the Lewis acid, we evaluated other aluminum-based Lewis acids. Both  $Et_3Al$  and

Scheme 1. Energy Transfer Sensitization Leading to Photocycloaddition of Maleimides 1a,b with Alkenes 2a-c,h



<sup>&</sup>lt;sup>a</sup>NMR yields. <sup>b</sup>Isolated yields. For clarity, hydrogens are not displayed in the single-crystal XRD structure of 3d.

Scheme 2. Photoreactivity of Maleimide 1a with Alkene 2a in the Presence of Lewis Acid (Top) and in the Presence of Both the Lewis Acid and Thioxanthone Photosensitizer (Bottom)

## Lewis Acid Photocatalysis

Table 1. Optimization of Photoreactivity of Maleimide 1a in the Presence of Lewis Acids and Thioxanthone



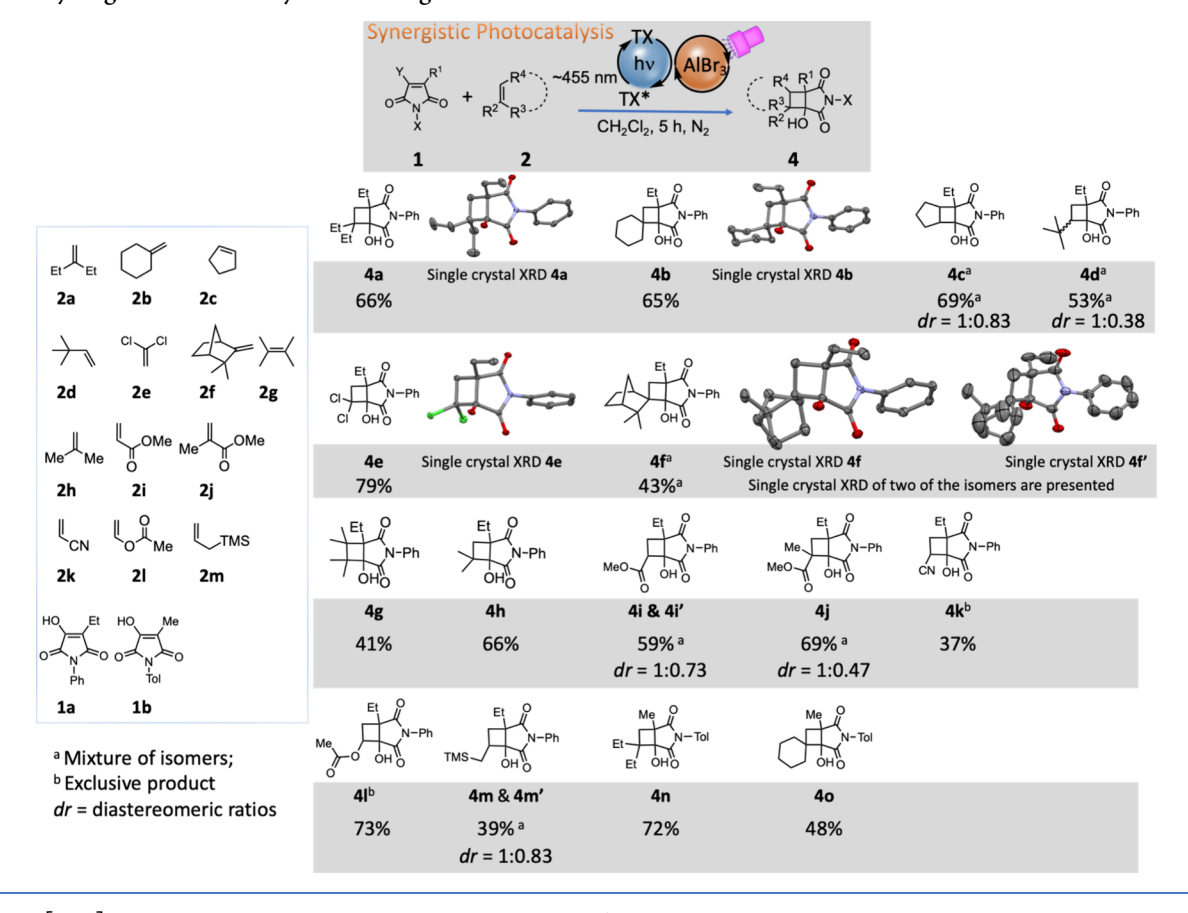
entry	variation from standard conditions	4a isolated yield (%)
1	standard conditions (LA = $AlBr_3$ )	66
2	standard conditions ( $LA = AlCl_3$ )	74
3	standard conditions (LA = $BF_3.OEt_2$ )	9
4	standard conditions (LA = $Et_3Al$ )	8
5	standard conditions (LA = $Et_2AlCl$ )	10
6	standard conditions (LA = $BCl_3$ )	56
7	standard conditions (LA = $Sc(OTf)_3$ )	-
8	standard conditions $(LA = Ti(OEt)_4)$	-
9	standard conditions (no light)	-
10	standard conditions (solvent: CHCl <sub>3</sub> )	55
11	50 mol % TFA, 10 mol % TX, CH <sub>2</sub> Cl <sub>2</sub> , blue LED, 12 h	-
12	50 mol % TFA, 10 mol % TX, $CH_2Cl_2$ , ~350 $\pm$ 30 nm, 12 h	-
13	$CH_2Cl_2$ , no LA, no TX, ~350 $\pm$ 30 nm, 12 h	-

Et<sub>2</sub>AlCl gave the identical photoproduct 4a in 8% and 10% isolated yields respectively (Table 1, entries 4 and 5). Nonchelating Lewis acid BCl<sub>3</sub> resulted in lowering of the yield from 74% to 56% isolated yield (Table 1, entry 6). Lewis acids such as Sc(OTf)<sub>3</sub> and Ti(OEt)<sub>4</sub> did not result in photoproduct (Table 1, entries 7 and 8). Direct irradiation at  $\sim$ 350  $\pm$  30 nm in the absence of both Lewis acid and thioxanthone did not result in photoproduct (Table 1, entry 13). In the absence of light from the standard conditions, no observable product was seen in the reaction, reinforcing the fact that the reaction originates from the excited state (Table 1, entry 9). Changing the solvent from dichloromethane to chloroform resulted in a slight drop in the isolated yield of the photoproduct 4a to 55% from 66% (Table 1, compare entries 1 and 10). Photoirradiation in the presence of trifluoroacetic acid serving as the Brønsted acid (both at blue LED and ~350

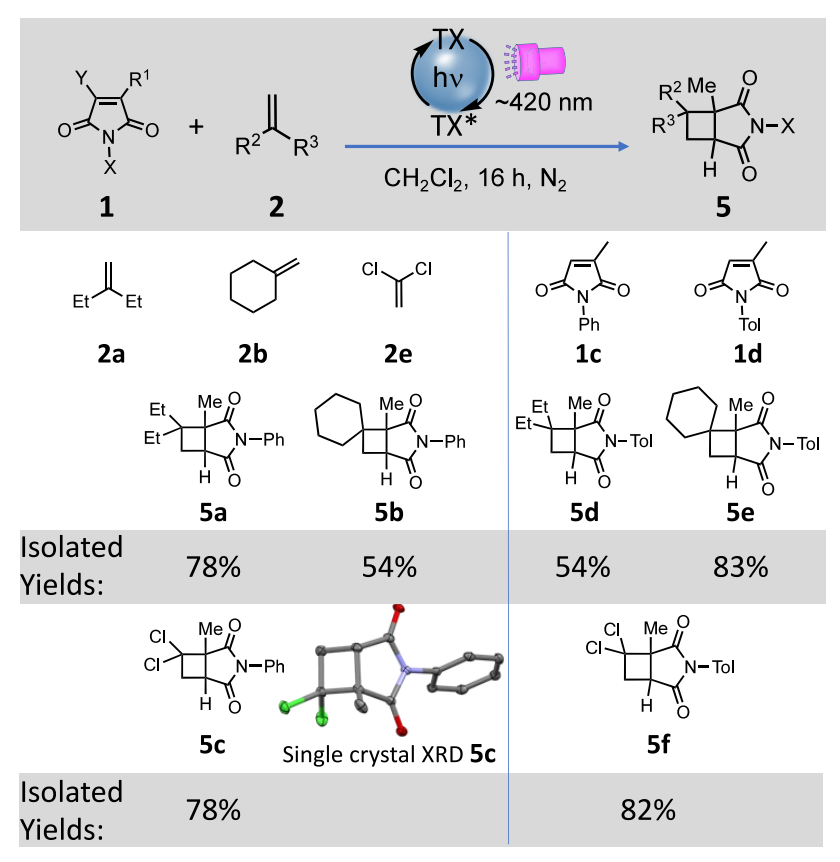
 $\pm$  30 nm) did not yield the desired photoproduct (Table 1, entries 11 and 12), showcasing the need for the Lewis acid to promote the reaction.

With optimized conditions using 50 mol % Lewis acid and 10 mol % of the thioxanthone sensitizer under blue LED irradiation for 5 h in dichloromethane at room temperature, we then evaluated the generality of the Lewis acid promoted photochemical transformation by changing both the maleimide and the alkene (Scheme 3). In the first set of experiments, we employed hydroxy maleimide 1a and systematically changed the type of alkene from 2a to 2f (Scheme 3, left) under synergistic photocatalytic conditions. Blue LED irradiation of 1a with methylenecyclohexane 2b with thioxanthone and AlBr<sub>3</sub> in CH<sub>2</sub>Cl<sub>2</sub> for 5 h (standard conditions) led to 65% isolated yield of the photoproduct 4b. Changing the alkene from 1,1-disubstituted to 1,2-disubstituted alkene did not significantly

Scheme 3. Synergistic Photocatalysis Involving Maleimides and Alkenes



Scheme 4. [2+2]-Photocycloaddition Involving Maleimides 1c/d with Alkenes



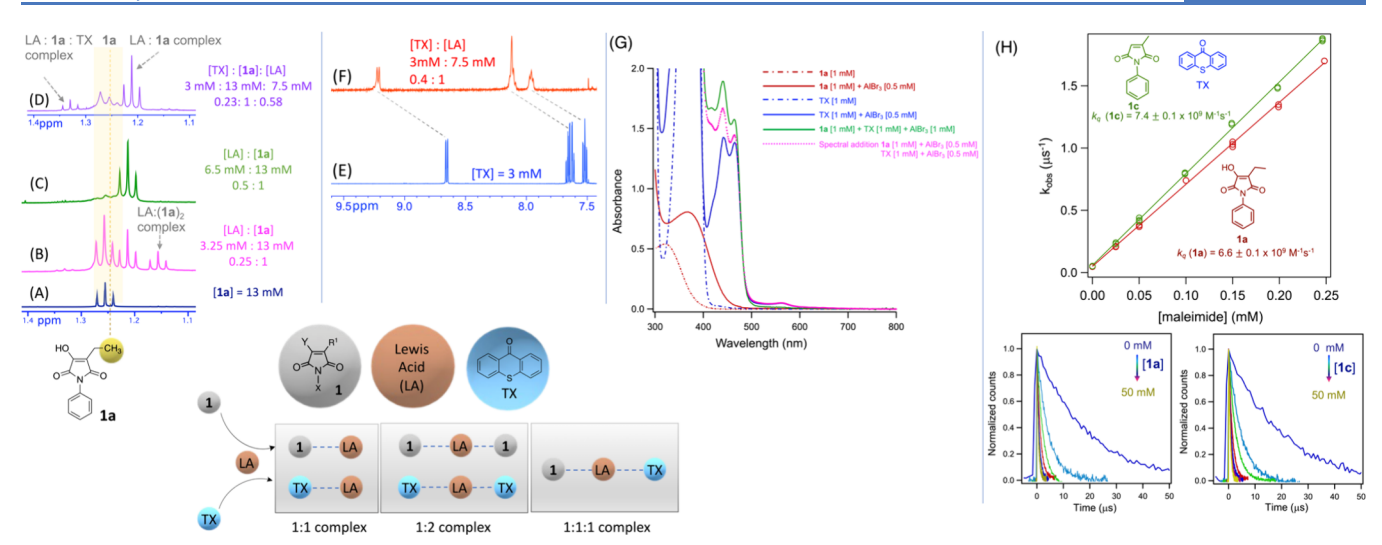


Figure 2.  $^{1}$ H NMR spectroscopy in CDCl<sub>3</sub> (left) and UV—vis spectroscopy (middle) to understand synergistic photocatalysis. The dotted line in UV—visible absorbance profile corresponds to hydroxy maleimide (1a, red dotted trace) and thioxanthone (TX, blue dotted trace) in dry dichloromethane at room temperature. The solid line in the UV—visible absorbance profile correlates with complexed 1a with AlBr<sub>3</sub> (red solid trace) and TX with AlBr<sub>3</sub> (blue solid trace), 1a+TX with AlBr<sub>3</sub> (green solid trace), and spectral addition of 1a+TX+AlBr<sub>3</sub> (pink dotted trace). Right: Determination of the bimolecular quenching rate constants  $k_q$  of quenching of thioxanthone triplet states by 1a or 1c using laser flash photolysis ( $\lambda_{\rm ex}$  = 355 nm, 7 ns pulse width). Triplet absorption decay rate constant monitored at 620 nm vs the concentration of 1a or 1c in argon-saturated acetonitrile solutions.

alter the photoproduct yield. For example, blue LED irradiation of 1a with cyclopentene 2c under standard irradiation conditions (Scheme 3) led to 69% isolated yield of the corresponding photoproduct 4c (mixture of isomers). Employing monosubstituted alkene 2d under the standard conditions led to 53% isolated yield of the photoproduct 4d (mixture of isomers). The reaction was also tolerant to haloalkenes with 79% isolated yield of the photoproduct 4e upon employing 1,1-dichloroethylene 2e. Synergistic photocatalysis was also effective with bicyclic alkene 2f, which gave 43% isolated yield of the photoproduct 4f (mixture of isomers). To explore the reactivity of functional alkenes, which are useful synthetic building blocks, we employed readily available alkenes 2g-o (Scheme 3). Photoreaction with maleimide 1a under synergistic photocatalytic conditions with tetramethylethylene (2g) and isobutene (2h) resulted in the corresponding photoproducts 4g and 4h in 41% and 66% isolated yields, respectively. To showcase the versatility of the employed photocatalytic system, we used easily accessible methacrylate (2i), methyl methacrylate (2j), and acrylonitrile (2k) as an alkene partner. Photoreaction with maleimide 1a under synergistic photocatalytic conditions with alkenes 2i-k led to the corresponding photoproduct 4 with 59%, 69%, and 37% isolated yields. Photoreaction with maleimide 1a under synergistic photocatalytic conditions with vinyl acetate 21 resulted in photoproduct 4l with 73% isolated yield. A point to note is that in the acrylate system the diastereomeric ratio (dr)was 1:0.73 in the photoproduct 4i and 1:0.47 in photoproduct 4j, while complete diastereocontrol was observed with vinyl acetate photoproduct 4l. Employing allyl silane 2m as the reactive partner for 1a under synergistic photocatalytic conditions led to the corresponding cyclobutane photoproduct 4m/4m' with an overall yield of 39%, showcasing substituent tolerance (trimethylsilane; TMS) under the reaction conditions (Scheme 3). Thus, the system was amenable to a broad scope of substrates. To assess the influence of the maleimide substituent, we evaluated maleimide 1b with alkenes 2a and 2b

under standard conditions (Scheme 3, right), which gave the corresponding photoproducts **4n** and **4o** in 72% and 48% yields, respectively.

To elucidate the structural features of the maleimide that is responsible for the observed chemoselectivity, we evaluated maleimides 1c and 1d, which lack the hydroxy substituent on the maleimide skeleton. Photoirradiation at  $\sim$ 420  $\pm$  30 nm (16 h irradiation) of maleimide 1c/d with alkene 2a/2b/2e with TX as a photosensitizer led to an efficient reaction leading to corresponding photoproduct 5 in isolated yields varying from 54% to 83% (Scheme 4). The photoproduct structures were deciphered by NMR spectroscopy and HRMS.<sup>35</sup> Unambiguous characterization of the photoproduct 5c was established by single-crystal XRD.<sup>35</sup> Closer inspection of the photoproduct 4 (derived from hydroxy maleimides 1a/b) and photoproduct 5 (derived from maleimides 1c/d, lacking the hydroxy substituent) shows that regiochemistry was profoundly impacted by the presence/absence of the hydroxy substituent on the maleimide skeleton. For example, photoirradiation at  $\sim$ 420  $\pm$  30 nm (16 h irradiation) of maleimide 1c and alkene 2a with TX as a photosensitizer resulted in photoproduct 5a (78% isolated yield; Scheme 4), featuring a 1,2-relation between the gem-diethyl substituent and the bridge head methyl substituent. On the other hand, photoreactivity of hydroxy maleimide 1a and 2a in the presence of AlCl<sub>3</sub> and TX resulted in photoproduct 4a (74% isolated yield; Table 1, entry 2), featuring a 1,3-relation between the gem-diethyl substituent and the bridge head ethyl substituent. It was clear that the regiochemistry of photocycloaddition in maleimides can be manipulated by employing Lewis acids.

To understand the intricacies of Lewis acid mediated control of excited state transformations involving maleimides, we utilized <sup>1</sup>H NMR and UV—vis spectroscopic investigations to appreciate the mechanistic details of the process (Figure 2).<sup>35</sup> Addition of Lewis acid to hydroxy maleimide 1a led to complexation as revealed by the change in the proton resonance peaks (Figure 2A) of 1a. We utilized the ethyl

Scheme 5. Mechanistic Rationale for the Observed Divergence in Energy Transfer and Electron Transfer vs Lewis Acid Mediated Photocatalysis

group resonances in 1a as an NMR handle to gauge the interactions between 1a and AlBr<sub>3</sub> (Figure 2A–D). The triplet centered around 1.25 ppm (Figure 2A) changed upon addition of various amounts of the Lewis acid. Upon employing 0.5 equiv or higher amount of AlBr3, a triplet resonance centered around 1.22 ppm (Figure 2C) was observed that was upfield shifted when compared to the triplet resonance of the uncomplexed maleimide 1a (triplet resonance at 1.25 ppm). When less than 0.5 equiv of Lewis acid was employed, three distinct triplet resonances were observed (Figure 2B), which were tentatively assigned to the presence of uncomplexed 1a at 1.25 ppm, 1a@AlBr<sub>3</sub> complex at 1.22 ppm, and (1a)<sub>2</sub>@AlBr<sub>3</sub> complex at 1.15 ppm. In addition, the OH resonance of 1a disappeared upon addition of the Lewis acid, indicating that the OH group was critical for Lewis acid complexation with maleimide (SI Figure S109).35 Similarly, addition of Lewis acid to thioxanthone led to complexation, as revealed by the change in the thioxanthone proton resonances (Figure 2E,F). For example, the aromatic resonances centered around 7.6 and 8.6 ppm (Figure 2E) were shifted to ~8.0 and ~9.1 ppm (Figure 2F), respectively.

The interaction of a Lewis acid with hydroxy maleimide 1a was further ascertained by a bathochromic shifted absorption (Figure 2G) in the presence of the Lewis acid (absorption spectra ending at ~480 nm in the presence of AlBr<sub>3</sub> when compared to ~390 nm in the absence of AlBr<sub>3</sub>). Similarly, the interaction of a Lewis acid with thioxanthone (TX@AlBr<sub>3</sub>) was ascertained from the bathochromic shift in the absorption (Figure 2G) in the presence of the Lewis acid (absorption spectra ending at ~592 nm in the presence of AlBr<sub>3</sub> when compared to ~420 nm in the absence of AlBr<sub>3</sub>). Addition of a Lewis acid to a mixture of thioxanthone and la showed that there is likely a synergistic interaction between them, leading to a ternary complex involving 1a, AlBr<sub>3</sub>, and TX (Figure 2D). This conjecture is based on our observation of the <sup>1</sup>H NMR resonance of the methyl functionality in 1a. When compared to the uncomplexed maleimide 1a methyl triplet resonance centered around 1.25 ppm (Figure 2A) and the upfield shifted resonance for both 1a@AlBr<sub>3</sub> and (1a)<sub>2</sub>@AlBr<sub>3</sub> complexes (Figure 2B,C), the methyl triplet resonance was downfield shifted to around 1.32 ppm (Figure 2D) for the ternary

complex involving 1a, AlBr3, and TX. In addition, the methyl resonances were broadened (Figure 2D), indicating that there is a dynamic exchange occurring in the system within the NMR time scale. Based on these observations, we believe that there is a synergistic interaction between the Lewis acid (AlBr<sub>3</sub>), thioxanthone, and 1a. This conjecture is once again bolstered by our UV-vis studies, where the absorption spectra of 1a and TX in the presence AlBr<sub>3</sub> (Figure 2G) were distinct when compared to 1a with AlBr3 and TX. A closer examination of the absorption spectra (Figure 2G) indicates that the UV-vis spectrum of the Lewis acid-substrate-thioxanthone (green trace in Figure 2G) has distinct absorption features and intensities when compared to the UV-vis of Lewis acidsubstate (solid red trace in Figure 2G), Lewis acidthioxanthone (solid blue trace in Figure 2G), and the mathematical additive features of the individual complexes (Lewis acid-substrate and Lewis acid-thioxanthone; pink dotted trace in Figure 2G). It is our conjecture that a ternary complex featuring Lewis acid-substrate-thioxanthone likely coexists (dynamically) with Lewis acid-substrate and Lewis acid-thioxanthone complexes in solution. Examination of the transition centered at ~440 and ~465 nm observed with the TX@AlBr3 complex showed a hyperchromic effect when the UV-vis spectrum was recorded for the mixture of 1a with AlBr<sub>3</sub> and TX (Figure 2G). Thus, <sup>1</sup>H NMR and UV-vis spectroscopic investigations likely point to the involvement of a 1a-AlBr<sub>3</sub>-TX complex in addition to the 1a-AlBr<sub>3</sub> complex and TX-AlBr<sub>3</sub> complex under our reaction conditions. We also ascertained that photoinduced electron transfer in the system is endergonic, and hence the reaction likely proceeds via energy transfer. 35,40-42

As we employed thioxanthone as the photosensitizer for the reaction involving 1a (Scheme 1) and 1c (Scheme 4), we utilized transient absorption measurements to ascertain the rate constant for triplet energy transfer. Laser excitation ( $\lambda_{\rm ex}$  = 355 nm, pulse width = 7 ns) of an argon-saturated solution of TX in acetonitrile generated a triplet transient absorption spectrum, which was in agreement with previously published reports. This triplet absorption of TX centered at ~620 nm was quenched by 1a, leading to the formation of triplet 1a, i.e.,  $^31a^*$ , with a bimolecular quenching rate constant  $k_q^{-1a} = (6.6 \pm$ 

 $0.1) \times 10^9~{\rm M}^{-1}~{\rm s}^{-1}$  (Figure 2H). Similarly, the triplet of TX was quenched by 1c, leading to the formation of triplet 1c, i.e.,  ${}^3{\bf 1c}^*$ , with a bimolecular quenching rate constant  $k_{\rm q}^{\ 1c} = (7.4 \pm 0.1) \times 10^9~{\rm M}^{-1}~{\rm s}^{-1}$  (Figure 2H). The near diffusion control rate constant for triplet energy transfer from TX to maleimides 1a and 1c shows that generation of the corresponding triplet excited maleimide is an efficient process.

Based on our photochemical investigations,<sup>35</sup> we propose the likely mechanistic pathway for the observed divergence in energy transfer vs Lewis acid mediated photocatalysis involving maleimides. In the presence of Lewis acid, hydroxy maleimides 1a/b form dynamic complexes 44,45 that can be excited either by directed irradiation (bathochromically shifted absorption) or by triplet energy transfer (Scheme 5). While we have proposed the Lewis acid-substrate complex coexisting (dynamically) with Lewis acid-substrate-thioxanthone ternary complex, at the present time we cannot pinpoint which of the species plays a dominant role in substrate activation during the photocatalytic cycle. Irrespective of the species, the activation of maleimides with Lewis acid occurs through deprotonation of the OH bond, leading to unique excited state reactivity. The triplet excited Lewis acid-maleimide complex reacts with alkene 2 to form the triplet diradical TDR-4, which intersystem crosses to ZI-4 (via SDR-4) en route to the formation of the observed photoproduct 4. The triplet excited maleimide <sup>3</sup>[1ab]\*, featuring a hydroxy substituent (triplet excited maleimides 1a and 1b), undergoes addition with alkene 2 to form a 1,4-triplet diradical TDR-3, which rearranges to form a 1,5-triplet diradical TDR-3' followed by intersystem crossing to enol-3, which tautomerizes to form the observed photoproduct 3. At the present stage we cannot rule out the formation of a triplet exciplex leading to the formation of a radical-ion pair, RIP-3, that intersystem crossed to the zwitterion ZI-3<sup>46</sup> en route to the formation of photoproduct 3. An alternative pathway via a photoinduced electron transfer from excited triplet TX to maleimide was also evaluated. Based on redox potential, this electron transfer will be endergonic, making this pathway less likely. In the case of triplet excited maleimide <sup>3</sup>[1c]\*, which lacks a hydroxy substituent, undergoes addition with alkene 2 to form 1,4-triplet diradical TDR-5, which intersystem crosses to the singlet diradical SDR-5, leading to the formation of the observed photoproduct 5.

Thus, our study has showcased that one can judiciously manipulate the excited state chemistry with a combination of substrate, Lewis acid, and the sensitizer. The synergistic interactions between the three (i.e., substrate, Lewis acid, and the sensitizer) control both the chemoselectivity and the regioselectivity in the reaction. We are in the process of understanding how excited state dynamics impact the reactivity and efficiency in such systems so that the process can be generalized for a variety of photochemical transformations. This will have a profound impact on the development of Lewis acid mediated photocatalytic reactions and uncover new excited state pathways.

# ASSOCIATED CONTENT

## **5** Supporting Information

The Supporting Information is available free of charge at https://pubs.acs.org/doi/10.1021/acscatal.4c01185.

Experimental procedures, characterization data (<sup>1</sup>H and <sup>13</sup>C NMR spectroscopy, HRMS, XRD) of compounds,

electrochemical data, and photophysical measurements (PDF)

Single-crystal XRD data of 3d (CCDC # 2270025) (CIF)

Single-crystal XRD data of 4a (CCDC # 2270030) (CIF)

Single-crystal XRD data of 4b (CCDC # 2270028) (CIF)

Single-crystal XRD data of 4e (CCDC # 2270026) (CIF)

Single-crystal XRD data of 4f (CCDC # 2270029) (CIF)

Single-crystal XRD data of 4f' (CCDC # 2270322) (CIF)

Single-crystal XRD data of **5c** (CCDC # 2270027) (CIF)

#### AUTHOR INFORMATION

### **Corresponding Author**

Jayaraman Sivaguru — Center for Photochemical Sciences and Department of Chemistry, Bowling Green State University, Bowling Green, Ohio 43403, United States; orcid.org/0000-0002-0446-6903; Email: sivagj@bgsu.edu

#### Authors

Jayachandran Parthiban — Center for Photochemical Sciences and Department of Chemistry, Bowling Green State University, Bowling Green, Ohio 43403, United States; orcid.org/0000-0002-5916-1701

Dipti Garg – Center for Photochemical Sciences and Department of Chemistry, Bowling Green State University, Bowling Green, Ohio 43403, United States

Sapna Ahuja – Center for Photochemical Sciences and Department of Chemistry, Bowling Green State University, Bowling Green, Ohio 43403, United States

Steffen Jockusch — Center for Photochemical Sciences and Department of Chemistry, Bowling Green State University, Bowling Green, Ohio 43403, United States; orcid.org/0000-0002-4592-5280

Angel Ugrinov – Department of Chemistry and Biochemistry, North Dakota State University, Fargo, North Dakota 58103, United States

Complete contact information is available at: https://pubs.acs.org/10.1021/acscatal.4c01185

## **Author Contributions**

The manuscript was written through contributions of all authors. All authors have given approval to the final version of the manuscript.

#### Notes

The authors declare no competing financial interest.

## ACKNOWLEDGMENTS

This manuscript is dedicated to Prof. Thorsten Bach on the occasion of his 60th birthday. We thank Ms. Sandra George for help with the TOC graphic. We thank Mr. Atanu Ghosh for providing the IUPAC names of the compounds. S.A. thanks the Center for Photochemical Sciences and BGSU for the McMaster Fellowship (2019–2020). J.P. thanks the Center for Photochemical Sciences and BGSU for the Taller fellowship (2023-2024). The work was performed with generous support from the National Science Foundation to JS (CHE-1955524).

#### REFERENCES

- (1) Sheldon, R. A.; Woodley, J. M. Role of Biocatalysis in Sustainable Chemistry. *Chem. Rev.* **2018**, *118*, 801–838.
- (2) Wu, S.; Snajdrova, R.; Moore, J. C.; Baldenius, K.; Bornscheuer, U. T. Biocatalysis: Enzymatic Synthesis for Industrial Applications. *Angew. Chem., Int. Ed.* **2021**, *60*, 88–119.
- (3) Hönig, M.; Sondermann, P.; Turner, N. J.; Carreira, E. M. Enantioselective Chemo- and Biocatalysis: Partners in Retrosynthesis. *Angew. Chem., Int. Ed.* **2017**, *56*, 8942–8973.
- (4) Turro, N. J.; Ramamurthy, V.; Scaiano, J. C. A Theory of Molecular Organic Photochemistry. In *Modern Molecular Photochemistry of Organic Molecules*; University Science Books: Sausalito, CA, 2010; pp 319–382.
- (5) Genzink, M. J.; Kidd, J. B.; Swords, W. B.; Yoon, T. P. Chiral Photocatalyst Structures in Asymmetric Photochemical Synthesis. *Chem. Rev.* **2022**, *122*, 1654–1716.
- (6) Poplata, S.; Tröster, A.; Zou, Y.-Q.; Bach, T. Recent Advances in the Synthesis of Cyclobutanes by Olefin [2 + 2] Photocycloaddition Reactions. *Chem. Rev.* **2016**, *116*, 9748–9815.
- (7) Kumarasamy, E.; Ayitou, A. J.-L.; Vallavoju, N.; Raghunathan, R.; Iyer, A.; Clay, A.; Kandappa, S. K.; Sivaguru, J. Tale of Twisted Molecules. Atropselective Photoreactions: Taming Light Induced Asymmetric Transformations through Non-biaryl Atropisomers. *Acc. Chem. Res.* **2016**, *49*, 2713–2724.
- (8) Baburaj, S.; Valloli, L. K.; Parthiban, J.; Garg, D.; Sivaguru, J. Manipulating excited state reactivity and selectivity through hydrogen bonding from solid state reactivity to Brønsted acid photocatalysis. *Chem. Commun.* **2022**, *58*, 1871–1880.
- (9) Kandappa, S. K.; Ahuja, S.; Singathi, R.; Valloli, L. K.; Baburaj, S.; Parthiban, J.; Sivaguru, J. Using Restricted Bond Rotations to Enforce Excited-State Behavior of Organic Molecules. *Synlett* **2022**, 33, 1123–1134.
- (10) Nicewicz, D. A.; MacMillan, D. W. C. Merging Photoredox Catalysis with Organocatalysis: The Direct Asymmetric Alkylation of Aldehydes. *Science* **2008**, 322, 77–80.
- (11) Narayanam, J. M. R.; Tucker, J. W.; Stephenson, C. R. J. Electron-Transfer Photoredox Catalysis: Development of a Tin-Free Reductive Dehalogenation Reaction. *J. Am. Chem. Soc.* **2009**, *131*, 8756–8757.
- (12) Prier, C. K.; Rankic, D. A.; MacMillan, D. W. C. Visible Light Photoredox Catalysis with Transition Metal Complexes: Applications in Organic Synthesis. *Chem. Rev.* **2013**, *113*, 5322–5363.
- (13) Skubi, K. L.; Blum, T. R.; Yoon, T. P. Dual Catalysis Strategies in Photochemical Synthesis. *Chem. Rev.* **2016**, *116*, 10035–10074.
- (14) Alabugin, I. V.; Harris, T. Photoredox-Initiated Radical Cascades Enabling Collective Synthesis of 33 Natural Products. *Chem.* **2017**, *2*, 753–755.
- (15) Ghosh, I.; Shaikh, R. S.; König, B. Sensitization-Initiated Electron Transfer for Photoredox Catalysis. *Angew. Chem., Int. Ed.* **2017**, *56*, 8544–8549.
- (16) Lewis, F. D.; Howard, D. K.; Oxman, J. D. Lewis acid catalysis of coumarin photodimerization. *J. Am. Chem. Soc.* **1983**, *105*, 3344–5.
- (17) Lewis, F. D.; Barancyk, S. V. Lewis acid catalysis of photochemical reactions. 8. Photodimerization and cross-cyclo-addition of coumarin. *J. Am. Chem. Soc.* **1989**, *111*, 8653–8661.
- (18) Takasu, K.; Nagao, S.; Ihara, M. Synthesis of Medium-Sized Cyclic  $\gamma$ -Haloketones by Radical-Mediated Ring-Opening Reaction of Lewis Acid Catalyzed [2 + 2]-Cycloaddition Products. *Tetrahedron Lett.* **2005**, *46*, 1005–1008.
- (19) Görner, H.; Wolff, T. Lewis-acid-catalyzed Photodimerization of Coumarins and N-methyl-2-quinolone. *Photochem. Photobiol.* **2008**, 84, 1224–1230.
- (20) Guo, H.; Herdtweck, E.; Bach, T. Enantioselective Lewis acid catalysis in intramolecular [2 + 2] photocycloaddition reactions of coumarins. *Angew. Chem., Int. Ed.* **2010**, *49*, 7782–7785.
- (21) Stegbauer, S.; Jandl, C.; Bach, T. Chiral Lewis acid catalysis in a visible light-triggered cycloaddition/rearrangement cascade. *Chem. Sci.* **2022**, *13*, 11856–11862.

- (22) Blum, T. R.; Miller, Z. D.; Bates, D. M.; Guzei, I. A.; Yoon, T. P. Enantioselective photochemistry through Lewis acid—catalyzed triplet energy transfer. *Science* **2016**, *354*, 1391.
- (23) Daub, M. E.; Jung, H.; Lee, B. J.; Won, J.; Baik, M.-H.; Yoon, T. P. Enantioselective [2 + 2] Cycloadditions of Cinnamate Esters: Generalizing Lewis Acid Catalysis of Triplet Energy Transfer. *J. Am. Chem. Soc.* **2019**, *141*, 9543–9547.
- (24) Zheng, J.; Swords, W. B.; Jung, H.; Skubi, K. L.; Kidd, J. B.; Meyer, G. J.; Baik, M.-H.; Yoon, T. P. Enantioselective Intermolecular Excited-State Photoreactions Using a Chiral Ir Triplet Sensitizer: Separating Association from Energy Transfer in Asymmetric Photocatalysis. *J. Am. Chem. Soc.* **2019**, *141*, 13625–13634.
- (25) Wang, H.; Cao, X.; Chen, X.; Fang, W.; Dolg, M. Regulatory Mechanism of the Enantioselective Intramolecular Enone [2 + 2] Photocycloaddition Reaction Mediated by a Chiral Lewis Acid Catalyst Containing Heavy Atoms. *Angew. Chem., Int. Ed.* **2015**, *54*, 14295–14298.
- (26) Martinez-Haya, R.; Marzo, L.; König, B. Reinventing the De Mayo reaction: synthesis of 1,5-diketones or 1,5-ketoesters via visible light [2 + 2] cycloaddition of  $\beta$ -diketones or  $\beta$ -ketoesters with styrenes. *Chem. Commun.* **2018**, *54*, 11602–11605.
- (27) Jones, B. A.; Solon, P.; Popescu, M. V.; Du, J.-Y.; Paton, R.; Smith, M. D. Catalytic Enantioselective  $6\pi$  Photocyclization of Acrylanilides. *J. Am. Chem. Soc.* **2023**, *145*, 171–178.
- (28) Zhang, W.; Zhang, L.; Luo, S. Catalytic Asymmetric Visible-Light de Mayo Reaction by ZrCl4-Chiral Phosphoric Acid Complex. *J. Am. Chem. Soc.* **2023**, *145*, 14227–14232.
- (29) Zhang, W.; Luo, S. Visible-light promoted de Mayo reaction by zirconium catalysis. *Chem. Commun.* **2022**, *58*, 12979–12982.
- (30) Stegbauer, S.; Jeremias, N.; Jandl, C.; Bach, T. Reversal of reaction type selectivity by Lewis acid coordination: the ortho photocycloaddition of 1-and 2-naphthaldehyde. *Chem. Sci.* **2019**, *10*, 8566–8570.
- (31) Kumarasamy, E.; Raghunathan, R.; Jockusch, S.; Ugrinov, A.; Sivaguru, J. Tailoring Atropisomeric Maleimides for Stereospecific [2 + 2] Photocycloaddition—Photochemical and Photophysical Investigations Leading to Visible-Light Photocatalysis. *J. Am. Chem. Soc.* **2014**, *136*, 8729–8737.
- (32) Ahuja, S.; Jockusch, S.; Ugrinov, A.; Sivaguru, J. Energy Transfer Catalysis by Visible Light: Atrop- and Regio-Selective Intermolecular [2 + 2]-Photocycloaddition of Maleimide with Alkenes. *Eur. J. Org. Chem.* **2020**, 2020, 1478–1481.
- (33) Strieth-Kalthoff, F.; Henkel, C.; Teders, M.; Kahnt, A.; Knolle, W.; Gomez-Suarez, A.; Dirian, K.; Alex, W.; Bergander, K.; Daniliuc, C. G.; Abel, B.; Guldi, D. M.; Glorius, F. Discovery of Unforeseen Energy-Transfer-Based Transformations Using a Combined Screening Approach. *Chem.* **2019**, *5*, 2183–2194.
- (34) He, J.; Liu, Q. Highly Efficient Visible-Light-Driven [2 + 2] Cycloaddition of Maleimides to Alkenes and Alkynes for the Synthesis of 3-Azabicyclo[3.2.0]heptane-Fused Scaffolds. *Synthesis* **2022**, *54*, 925–942.
- (35) Refer to the Supporting Information.
- (36) Gerard, B.; Jones, G.; Porco, J. A. A Biomimetic Approach to the Rocaglamides Employing Photogeneration of Oxidopyryliums Derived from 3-Hydroxyflavones. *J. Am. Chem. Soc.* **2004**, *126*, 13620–13621.
- (37) Wang, W.; Clay, A.; Krishnan, R.; Lajkiewicz Neil, J.; Brown Lauren, E.; Sivaguru, J.; Porco John, A. Total Syntheses of the Isomeric Aglain Natural Products Foveoglin A and Perviridisin B: Selective Excited-State Intramolecular Proton-Transfer Photocycload-dition. *Angew. Chem., Int. Ed.* **2017**, *56*, 14479–14482.
- (38) Wen, S.; Boyce, J. H.; Kandappa, S. K.; Sivaguru, J.; Porco, J. A. Regiodivergent Photocyclization of Dearomatized Acylphloroglucinols: Asymmetric Syntheses of (–)-Nemorosone and (–)-6-epi-Garcimultiflorone A. J. Am. Chem. Soc. 2019, 141, 11315–11321.
- (39) Kandappa, S. K.; Kumarasamy, E.; Singathi, R.; Valloli, L. K.; Ugrinov, A.; Sivaguru, J. Chemoselective Photoreaction of Enamides: Divergent Reactivity towards [3 + 2]-Photocycloaddition vs Paternò—Büchi Reaction†. *Photochem. Photobiol.* **2021**, *97*, 1391–1396.

- (40) Farid, S.; Dinnocenzo, J. P.; Merkel, P. B.; Young, R. H.; Shukla, D.; Guirado, G. Reexamination of the Rehm—Weller Data Set Reveals Electron Transfer Quenching That Follows a Sandros—Boltzmann Dependence on Free Energy. J. Am. Chem. Soc. 2011, 133, 11580—11587.
- (41) Pavlishchuk, V. V.; Addison, A. W. Conversion constants for redox potentials measured versus different reference electrodes in acetonitrile solutions at 25°C. *Inorg. Chim. Acta* **2000**, 298, 97–102.
- (42) Dinnocenzo, J. P.; Feinberg, E. C.; Farid, S. Multiple Intermolecular Exciplexes in Highly Polar Solvents. *J. Phys. Chem. A* **2017**, *121*, 3662–3670.
- (43) Iyer, A.; Clay, A.; Jockusch, S.; Sivaguru, J. Evaluating brominated thioxanthones as organo-photocatalysts. *J. Phys. Org. Chem.* **2017**, *30*, No. e3738.
- (44) Chadda, S. K.; Childs, R. F. The use of homogeneous and heterogeneous Lewis acids to catalyse the photoisomerizations of phenols. *Can. J. Chem.* **1985**, *63*, 3449–3455.
- (45) Nishimoto, Y.; Nakao, S.; Machinaka, S.; Hidaka, F.; Yasuda, M. Synthesis and Characterization of Pheox— and Phebox—Aluminum Complexes: Application as Tunable Lewis Acid Catalysts in Organic Reactions. *Chem.—Eur. J.* **2019**, *25*, 10792–10796.
- (46) Salem, L.; Rowland, C. The Electronic Properties of Diradicals. Angewandte Chemie International Edition in English 1972, 11, 92–111.